

# Predicting the Scalp Potential Topography in the Multifocal VEP by fMRI

Shariful Islam<sup>1</sup>, Torsten Wüstenberg<sup>2</sup>, Michael Bach<sup>3</sup>, Dorothe A. Poggel<sup>1</sup>, Hans Strasburger<sup>1</sup>

<sup>1</sup>Dept. Medical Psychology U. Göttingen; <sup>2</sup>Charité Berlin; <sup>3</sup>Ophthalmology U. Freiburg

shariful@math.uni-goettingen.de • strasburger@uni-muenchen.de

**Introduction:** Visual evoked potential amplitude and polarity from localized stimuli depend on the subject's individual folding of the primary and secondary visual cortex confounding the VEP as a measure of neural activation. To cross-validate three non-invasive imaging approaches for primary visual areas, we aim to predict multifocal VEP amplitude on the scalp from retinotopic fMRI data. To obtain retinotopic information we stimulated the central visual field using dart board patterns (rings, wedges and segments) in both fMRI and EEG recordings. We aim to eventually predict multifocal evoked potential topography and EEG sources (mVEPs: orthogonal time-series stimulation allows decomposing single-electrode EEG signal into components attributable to each stimulus region).

**Stimuli:** Sequences of expanding phase-reversing rings and rotating wedges (classical retinotopic mapping). Stimulus images were generated with MATLAB; both the EEG and fMRI stimulation were performed using Presentation. For fMRI, stimuli were shown via MRI-compatible goggles (VisuStimDigital, Resonance Technology). EEG & mVEP stimuli were presented on a computer screen.



Fig. 1 Visual regions

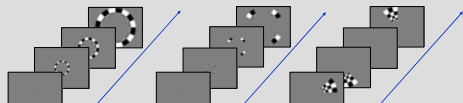


Fig. 2 Stimulus: Rings, Segments and Wedges

**Functional Magnetic Resonance Imaging (fMRI):** Siemens Trio 3T MRI scanner (GE-EPI, TR=2500, 28 slices, 2x2x2 mm<sup>3</sup> voxels, 5 stimulus cycles). Using the retinotopic mapping stimulus patterns (Fig. 2), corresponding activated regions on the visual cortex surface were determined. A high-resolution anatomical scan (T1-weighted) was acquired for segmentation of the white-gray matter border. Retinotopic maps were projected onto the cortical surface (Fig 3 & 4).

**fMRI Results:** Retinotopic mapping replicated findings from the literature (e.g. Wandell, 1999). Subregions within visual cortex could be defined based on visual field sign reversal in the polar angle retinotopic map. Segment stimulation generated circumscribed activated regions on visual cortex.

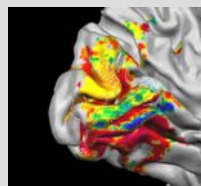


Fig. 3. Folded visual cortex on the left hemisphere with retinotopic activation; S; SI

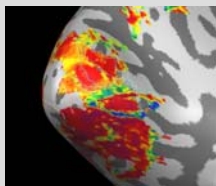


Fig. 4. Retinotopic polar angle map (inflated) with demarcated visual regions. S; SI

**Electroencephalography (EEG):** As one cross validation, source localization identified the brain areas generating activity from retinotopic stimulation (Fig. 2). EEG was recorded with BrainAmp MR+ Amplifier and Vision Recorder (62 channels, 500 Hz sampling rate), raw data pre-processing by Vision Analyzer (www.brainproducts.com). The signals were corrected for artifacts (eye movements or electrode drifts) and base-line corrected (mean level 50 ms prior to stimulus onset). Averages (VEPs) were computed separately for each stimulus position. Data were analyzed with the software CarTool<sup>4</sup> applying distributed localization techniques (Michel<sup>5</sup> et al. 2004). The figure below shows as example the VEP (500 ms) at the occipital lobe (O1, O2) for the first ring, first segment and first wedge, respectively.



Fig. 5. Averaged VEP at the occipital lobe for the ring, segment and wedge.

**EEG Results:** We used Cartool for source localization. The following figures depict electrode locations on a real head and preliminary non-constrained sources for sj. NS from a ring stimulus.

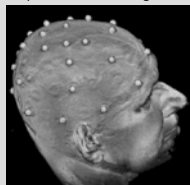


Fig. 6a. Electrode locations determined by anatomical MRI

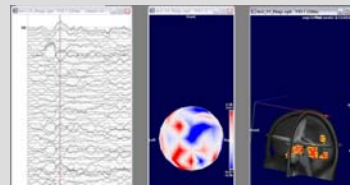


Fig. 6b. Ring stimulus. Left: all traces; right: Preliminary sources. S; NS

**Multifocal VEP (mVEP):** An mVEP of subject SI was recorded on a VerisScience system in Freiburg with reversal stimulation at 60 visual-field segments (Fig. 1). Electrodes were arranged in a "Southern Cross" on the inion. Data were Fourier low-pass filtered at 40 Hz, i.e. linear trend was removed, the spectrum obtained from a DFT, data above 40 Hz cut off, and data back-transformed to obtain the smoothed signal. Figure 7 & 8 show all traces in a Veris and Matlab matrix. S/N ratio in sj. SI was extremely low and we will need to repeat the measurements on another system.

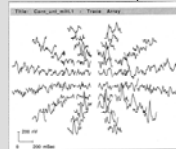


Fig. 7. mVEP Signals from Veris System; sj Co



Fig. 8 Low-pass filtered mVEP Signals; sj SI

**Matching VEP and mVEP Signals:** We cross-correlated an ideal VEP signal with the sixty mVEP signals to extract the latter's likely shape. The following figure shows a typical output:

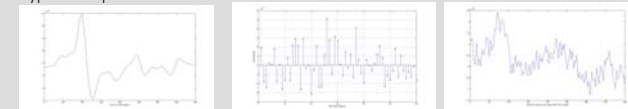


Fig. 9 'Ideal' VEP, cross-correlation result and 'best' matched mVEP signal

**Modelling – dipole location/orientation:** From anatomical MRI data we predict for a specified voxel the cortex surface orientation by a newly developed tool. From that we predict the head surface potential distribution by solving the forward problem (see box below). The two figures below show the potential distribution (left) of a certain generator and its location (small red point, right) and orientation (arrow) in the brain, respectively. The Cartesian coordinates in normalized units and the orientation of the generator can be obtained from the GUI. We will use the MNE suite for better result in the future.

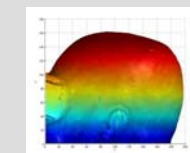


Fig. 10. Scalp potential distribution, sj, SI

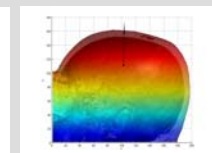


Fig. 11. Dipole location, sj, SI

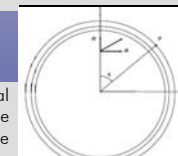


Fig. 12. GUI implementation

**Modelling – EEG forward problem:** To predict electrical activity at a specific electrode location from a dipole generator found in fMRI, EEG, or mVEP via a forward solution: For the simplest case, a three-shell concentric spherical head model, with a dipole located on the z-axis and a scalp point P located in the x-z plane (see figure below), the potential V at scalp point P generated by the dipole is given by (Hallez, 2007<sup>3</sup>):

$$V = \frac{1}{4\pi SR^2} \sum_{i=1}^{\infty} \frac{X(2i+1)^3}{g_i(i+1)^i} b^{i-1} [i d_r P_i(\cos\theta) + d_t P_i'(\cos\theta)],$$

where  $d_r$  and  $d_t$  are the dipole's radial and tangential components, respectively,  $R$  is the outer shell's radius,  $S$  the conductivity of scalp and brain tissue,  $X$  the ratio between the skull and soft tissue conductivity,  $b$  the relative distance of the dipole from the centre,  $\theta$  the polar angle of the surface point;  $P_i(\cdot)$  and  $P_i'(\cdot)$  are the Legendre polynomial and its associate, respectively,  $i$  is an index,  $i_1=2i+1$ ,  $r_1$  and  $r_2$  are the radius of the inner and the middle shell, respectively, and  $f_1 = r_1/R$ ,  $f_2 = r_2/R$ .



**Discussion:** Three highly different imaging methods allow linking neural generators with non-invasively obtained data: mVEP, fMRI, EEG. Area-V1 retinotopy with its highly systematic organization allows cross validating their results. This is **work in progress**. Four steps need to be solved: 1) Link of cortex-surface tool to fMRI retinotopy; 2) mVEP S/N ratio and polarity topography; 3) real-head forward model; 4) Coregistration of EEG (LAURA) sources and anatomical MRI. Our results are hoped to improve the validity of the VEP and EEG as an objective measure of visual brain activation.

## Acknowledgements

Funded by DFG grant „Multifocal VEP and Cortex Folding“ (STR 354/7-1) to HS  
We thank **PD Dr. Peter Dechent** and **Dr. Carsten Schmidt-Samoa** for help with MRI data acquisition and Presentation programming and **Brigitte Kurtz** for help with Cartool and EEG.

## References

- <sup>1</sup>Sutter E, Tran D (1992). The field topography of ERG components in man—II. The photopic luminance response. Vision Research 32, 433-446.
- <sup>2</sup>Neurobehavioral Systems, <http://www.neurobs.com/>
- <sup>3</sup>Hallez H et al (2007). Review on solving the forward problem in EEG source analysis. Journal of NeuroEngineering and Rehabilitation, 4:46 (29 pp).
- <sup>4</sup>Cartool, Functional Brain Mapping Laboratory, Geneva, Switzerland.
- <sup>5</sup>Michel CM, Murray MM, Lantz G, Gonzalez S, Spinelli L, Grave de Peralta R (2004). EEG source imaging. Clinical Neurophysiology 115, 2195-2222.